Laser Chem. Vol. 11, pp. 265–272
Reprints available directly from the Publisher
Photocopying permitted by license only

© 1991 Harwood Academic Publishers GmbH
Printed in Singapore

STEREODYNAMICAL STUDIES OF VELOCITY ALIGNED PHOTOFRAGMENTS

M. BROUARD, S. P. DUXON, P. A. ENRIQUEZ, R. SAYOS† and J. P. SIMONS

Chemistry Department, The University, Nottingham NG7 2RD, UK

The state resolved stereodynamics of bimolecular reactions can be probed using velocity aligned photofragments as reagents, and polarised, Doppler resolved laser detection techniques for the products. The new strategy and its application to the reaction $O(^1D) + N_2O \rightarrow NO + NO$ are outlined.

KEY WORDS: Stereodynamics, vector correlations, photodissociation.

1. INTRODUCTION

Polarised laser probing allows unprecedented levels of reagent state specification/selection and product state resolution and, with very narrow line lasers, of product velocity resolution *via* Doppler resolved spectroscopic techniques.[1–4] Such methods, first initiated for the stereodynamics of photodissociation, have now been extended to create a new experimental strategy for probing the stereodynamics of *bi*-molecular reactions.[5–7] Polarised photodissociation is used to generate superthermal "beams" of velocity aligned photofragments and the state-to-state stereodynamics of their subsequent collisions are probed at high resolution and sensitivity in a "simple" bulb experiment. The new strategy both complements and amplifies the more conventional molecular beam scattering technique. Doppler resolution of the polarised laser induced fluorescence (or ionisation) spectrum of the nascent *bi*-molecular collision products can allow determination of their quantum state distributions, scalar pair correlations *and* angular vector correlations, referenced initially to the laboratory frame, but after a simple laboratory to centre of mass transformation, to the *bi*-molecular collision frame.

The highly exothermic reaction

$$O(^1D) + N_2O \rightarrow NO + NO, \Delta E_O = 341 \text{ kJ mol}^{-1} \quad (1)$$

which follows the photodissociation of N_2O at 193 nm leads to the generation of rotationally excited and aligned NO molecules. The excitation into all vibrational levels up to and beyond the thermo-chemical limit of $v_{NO} = 16$ establishes the

† Present address: Departamento di Quimica Fisica, Universidad de Barcelona, 08028, Barcelona, Spain.

primary generation of superthermal, velocity aligned O(^{1}D) atoms.[17] The current status of our understanding of the reaction follows a brief outline of the basic theory for velocity aligned photofragment dynamics.

2. THEORY

Translation Alignment. Figure 1 shows the Newton diagram for the collision of a superthermal velocity aligned atom A with a stationary target molecule BC. The LAB frame is defined by the polarisation vector of the incident photolysis beam $\varepsilon_p \parallel Z$. The CM collision frame is defined by the collision velocity vector $\mathbf{k} \parallel z \parallel \mathbf{v}$, the photofragment recoil velocity; for a stationary target, $\mathbf{v} \parallel \mathbf{k} \parallel \mathbf{v}_{CM}$, the centre of mass velocity.

The LAB angular distribution of the *bi*molecular reaction products, AB, C, separating with a relative velocity $\mathbf{k}'$ is[5]

$$I(\hat{\varepsilon}_p \cdot \hat{\mathbf{k}}') \sim 1 + BP_2(\hat{\varepsilon}_p \cdot \hat{\mathbf{k}}') \tag{2}$$

The coefficient B, reflecting their LAB translational anisotropy is related to β, the reagent translational anisotropy, *via* the equation

$$B = \beta\langle P_2(\hat{\mathbf{k}} \cdot \hat{\mathbf{k}}')\rangle \equiv 5\langle P_2(\hat{\varepsilon}_p \cdot \hat{\mathbf{k}}')\rangle \tag{3}$$

Determination of the CM translational alignment $\langle P_2(\hat{\mathbf{k}} \cdot \hat{\mathbf{k}}')\rangle$ simply involves laboratory frame measurement of the product and reagent translational anisotropies. This can be done by using Doppler resolved laser induced fluorescence (or ionisation) spectroscopy, to probe the reaction products and the recasting of Eq. (2)

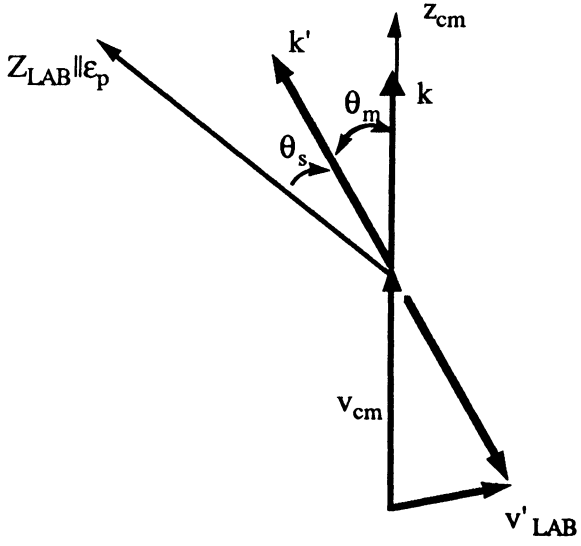

Figure 1 Schematic Newton diagram for the collision of superthermal velocity aligned atoms, with a stationary target molecule.

in terms of the spectral lineshape function[2]

$$g(\bar{v}) \sim 1 + \beta P_2(\hat{\varepsilon}_p \cdot \hat{\mathbf{k}}_a) P_2(\chi_D) \tag{4}$$

$\mathbf{k}_a$ represents the probe laser wave vector and χ_D, the relative displacement from the line centre, is defined as

$$\chi_D = \left(\frac{\bar{v} - \bar{v}}{\bar{v}_O}\right)\frac{c}{v} \equiv \frac{\bar{v} - \bar{v}_O}{\Delta\bar{v}_D} \tag{5}$$

Rotational alignment. The classical angular distribution of reaction product rotational vectors, $\mathbf{j}'$ is†

$$I(\hat{\varepsilon}_p \cdot \hat{\mathbf{j}}') \sim 1 + A P_2(\hat{\varepsilon}_p \cdot \hat{\mathbf{j}}') \tag{6}$$

where

$$A = \beta\langle P_2(\hat{\mathbf{k}} \cdot \hat{\mathbf{j}}')\rangle = 5\langle P_2(\hat{\varepsilon}_p \cdot \hat{\mathbf{k}}')\rangle \tag{7}$$

In terms of the rotational alignment parameter $A_O^{(2)}$, conventionally defined as[2,8]

$$A_O^{(2)}(\text{LAB}) \equiv 2\langle P_2(\hat{\varepsilon}_p \cdot \hat{\mathbf{j}}')\rangle \quad \text{or} \quad A_O^{(2)}(\text{CM}) \equiv 2\langle P_2(\hat{\mathbf{k}} \cdot \hat{\mathbf{j}}')\rangle \tag{8}$$

the alignment coefficient

$$A \equiv \frac{5}{2} A_O^{(2)}(\text{LAB}) \equiv \frac{1}{2}\beta A_O^{(2)}(\text{CM}) \tag{9}$$

in the high j limit.

In practice, estimation of the translational anisotropy and rotational alignment parameters B and A *via* simulation of the experimental Doppler profiles, requires several levels of convolution, to accommodate the probe laser line profile, the thermal motion of the precursor and target molecules and any spread in the superthermal reagent speeds introduced by the dynamics of the primary photodissociation process.[6]

Other vector correlations. Doppler resolved probing of photoninitiated *bi*-molecular collision/reaction products can reveal several additional correlations. As with direct photodissociation a total of nine bipolar moments are required to characterise fully the correlated angular distributions of $\mathbf{j}'$ and $\mathbf{k}'$ about ε_p, in a linearly polarised pump-probe experiment.[2] Provided the reagent translational anisotropy is known, the distributions of $\mathbf{j}'$ and $\mathbf{k}'$ can be referenced to the $\mathbf{k}$ vector rather than ε_p or the transition dipole μ and the Doppler profiles can be analysed to obtain the full set of bipolar moments.[2] Note however, the important correlation $\mathbf{k}'$, $\mathbf{j}'$, reflecting angle bending torques at the transition state, is invariant to the LAB → CM transformation.

3. STEREODYNAMICS OF THE REACTION $O(^1D) + N_2O \rightarrow NO + NO$

Quantum State Distributions and Scalar Pair Correlations

Photodissociation of N_2O at 193 nm initiates the highly exothermic reaction

$$O(^1D) + N_2O \rightarrow NO + NO \tag{10}$$

† In Eqs. (3) and (7) the factor $\beta/5$ may be equated with $\langle P_2(\hat{\varepsilon}_p \cdot \hat{\mathbf{k}})\rangle$, arising from the LAB → CM transformation.

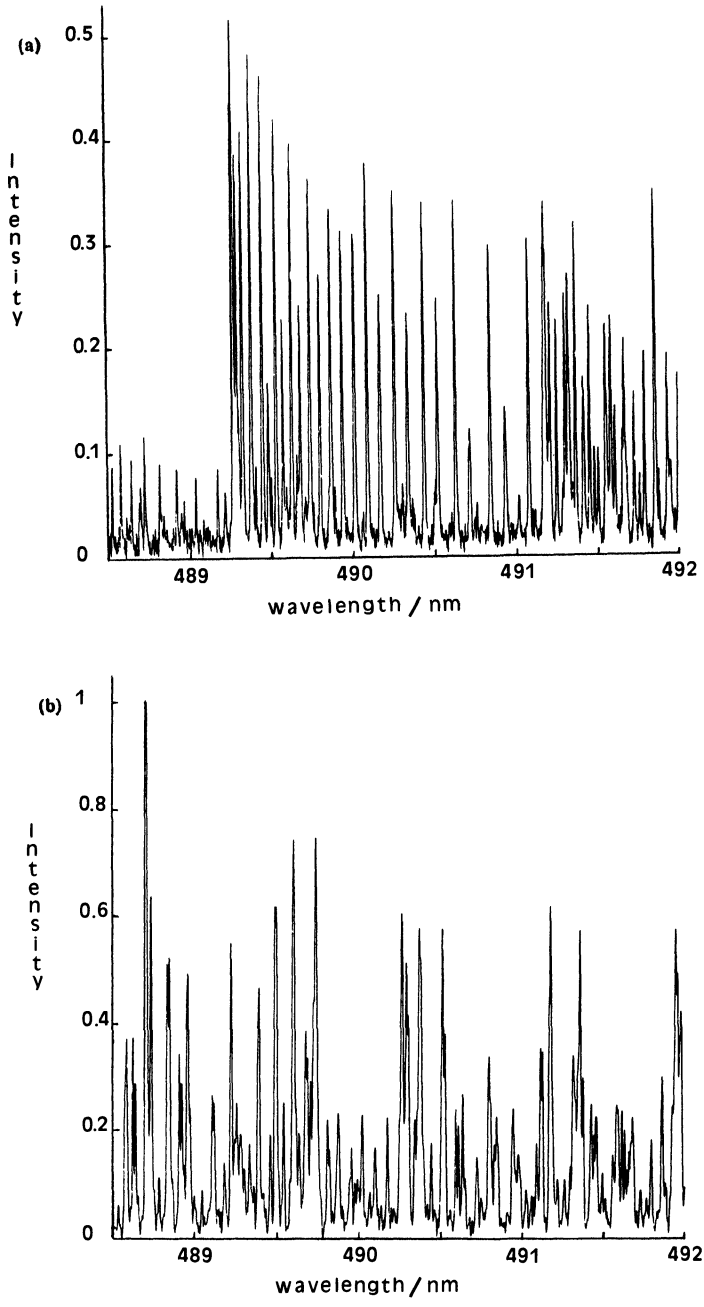

Figure 2 LIF spectra of NO($v = 17$) recorded under (a) relaxed, and (b) near single collision conditions.

which proceeds with near unit collision efficiency to generate NO molecules in a very broad spectrum of rovibrational states up to and including $v_{NO} = 18$.[7] Fully dispersed LIF spectra of NO have been recorded under both single collision and partially relaxed conditions, *via* the γ ($v \leqslant 12$) and $\beta(10 \leqslant v \leqslant 18)$ band systems. Full assignment of the populated levels is a daunting task, because of the very broad and dense rovibrational product state distributions (see Figure 2) but the task is now largely complete. Apart from those in the level $v = 0$ (*vide infra*) they are all endowed with high levels of rotational excitation (see Figure 2). Population of the most highly excited molecules, i.e. those generated in $v = 18$ two quanta above the thermochemical limit, require a collision energy $\langle E_{CM} \rangle \leqslant 70$ kJ mol^{-1}. This can only be introduced *via* the translational excitation of the reagent O(^{1}D) atoms generated in the primary photo-dissociation step.

$$N_2O + h\nu(193 \text{ nm}) \rightarrow N_2(v, J) + O(^1D) \qquad (11)$$

If the N_2 were formed predominantly in $v_{N_2} = 0$, for $\langle E_{CM} \rangle \leqslant 70$ kJ mol^{-1} energy conservation would require the primary excitation of the N_2 into rotational levels $J \leqslant 90$, accounting for $\leqslant 55\%$ of the available energy.† The analogous photodissociation of the isoelectronic molecule HN_3 generates N_2 in $v_{N_2} = 0$ with $\sim 50\%$ of the available energy in rotation.[9,10] Molecules generated in $v_{NO} = 0$ are rotationally cold (mean rotational temperatures $T_R \simeq 320$ K—see Figure 3) *and* translationally unexcited (Doppler with $\Delta\bar{\nu}_D = 0.044$ cm^{-1}—equivalent to a LAB kinetic energy ~ 110 cm^{-1}—see Figure 4). NO molecules in levels $v \geqslant 1$ are rotationally highly excited; e.g. those in $v = 1$ have a rotational temperature, $T_R \sim 5500$ K, those in higher vibrational levels appear to be even hotter. They also carry higher translational excitation (see Figure 4). These data allow estimates of the mean energy disposals and by energy conservation, of the scalar pair correlations summarised in *Table 1*.

The exceptionally cold distribution in NO($v = 0$) requires that it be partnered by NO molecules carrying very high levels of internal excitation, predominantly in the "super-excited" levels $16 \leqslant v_{NO} \leqslant 18$. The narrow spread in the Doppler profiles of NO($v = 0$), reflects a narrow spread in the internal energy of the excited partner; the broad distribution over internal rovibrational levels in NO($16 \leqslant v \leqslant 18$) must reflect the spread of collision energies in the hot atom reaction. A "near-stripping" mechanism for the channel leading to NO($v = 0$) would accord with the behaviour observed.

The NO molecules produced in levels $v = 1$–3 must also be accompanied by highly excited partners but the dramatic jump in their rotational and translational energies suggests the operation of an alternative dynamical pathway. High internal excitation in *both* NO partners suggests the operation of a short-lived complex mechanism: this view is reinforced by the absence of any measureable translational vector correlation, $\langle P_2(\hat{\mathbf{k}} \cdot \hat{\mathbf{k}}') \rangle \simeq 0$ (see below).

† A direct measurement of the discussion dynamics by Huber's group gives $\langle (E_{int}(N_2) \rangle = 58\%$, and $\beta[O(^1D)] = +0.48$ (P. Felder, B.-M. Haas and R. Huber, private communication).

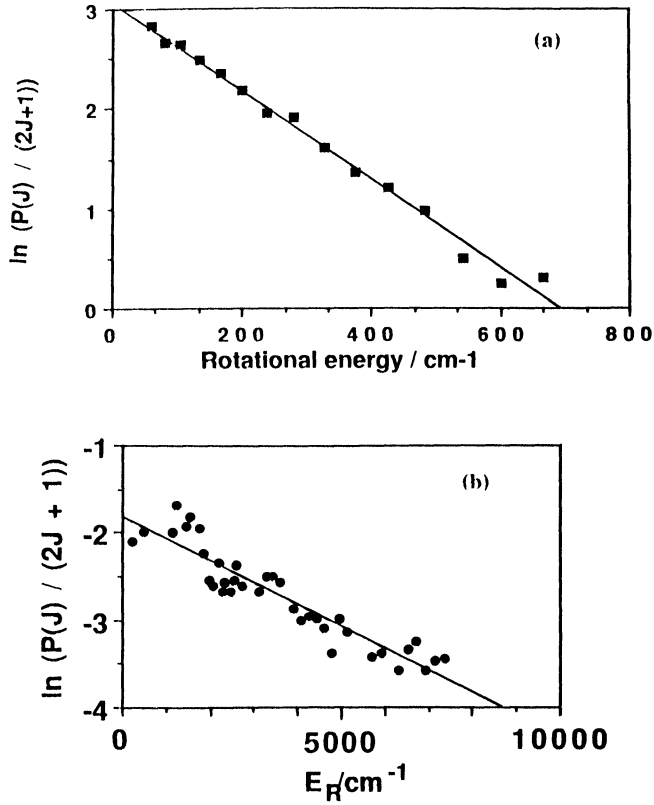

Figure 3 Rotational population distributions in NO; (a) $v = 0$; (b) $v = 1$.

Vector correlations. The LAB rotational alignments, $A_O^{(2)}$(LAB) for NO($v = 0$) are shown in Figure 5; despite the (inevitable) scatter, they are all negative, with $A_O^{(2)}$ (LAB) ~ -0.1. Assuming the product alignment $\langle P_2(\hat{\mathbf{k}} \cdot \hat{\mathbf{j}}')\rangle > 0$, the photofragment alignment must be positive, with $2 \geq \langle\beta\rangle \geq \frac{1}{2}$.† If the cold ("old") NO($v = 0$) were a spectator in a pure stripping reaction, no alignment would be expected; there must be some residual interaction between the two NO species at the transition state. The negative alignment could be introduced by reagent orbital angular momentum transfer.

A near stripping mechanism requires $\hat{\mathbf{k}} \cdot \hat{\mathbf{k}}' \sim 1$, and a LAB translational alignment B[NO] $\simeq \langle\beta[O(^1D)]\rangle$ (cf. Eq. (3)). The $\hat{\mathbf{k}},\hat{\mathbf{k}}'$ correlation can be estimated from the Doppler profiles; the rotational lines in the slow moving NO($v = 0$) are too narrow for the experimental resolution to reveal any changes in line shape when the excitation-detection geometry is changed from coaxial to perpendicular but their

† A direct measurement of the discussion dynamics by Huber's group gives $\langle(E_{int}(N_2)\rangle = 58\%$, and $\beta[O(^1D)] = +0.48$ (P. Felder, B.-M. Haas and R. Huber, private communication).

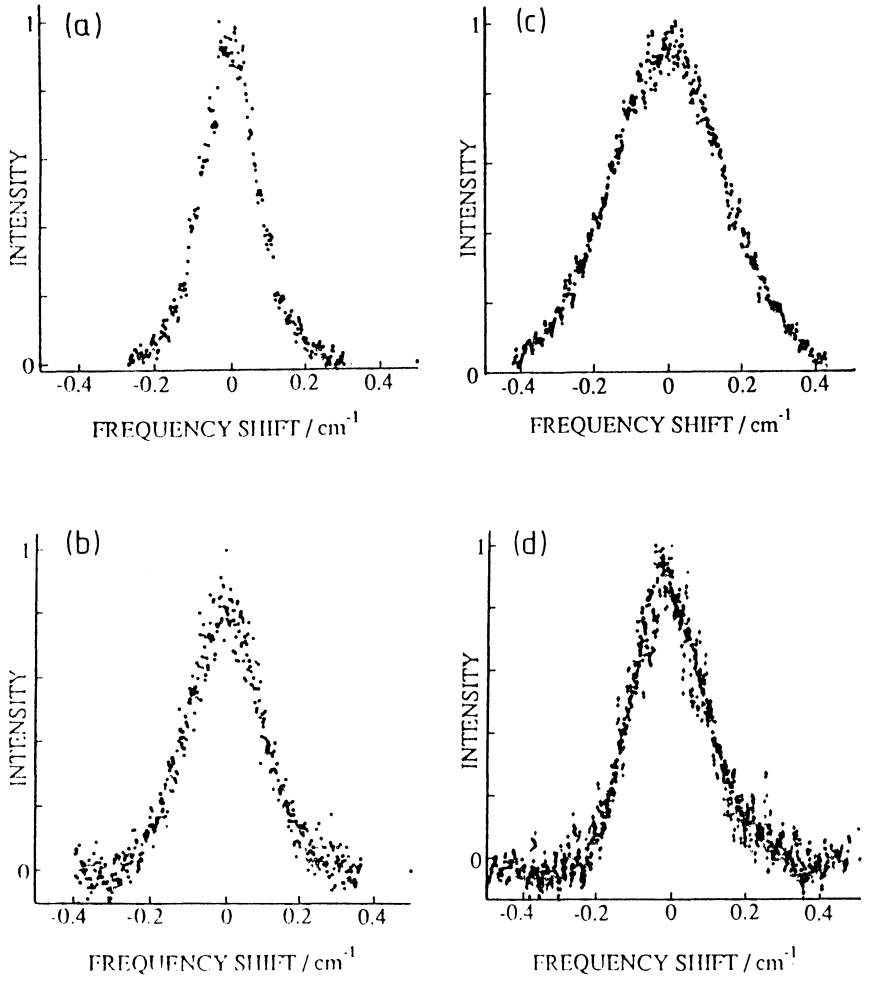

Figure 4 Doppler profiles for NO (a) $v = 0$, N = 20; (b) $v = 1$, N = 35; (c) $v = 3$, N = 31; all Case A; (d) $v = 10$, N = 26; Case A—circles, Case D—crosses.

Table 1 Energy disposal and pair correlations

$NO(v_1)$	E_v, cm^{-1}	$\langle E_R \rangle / cm^{-1}$	$\langle E_T \rangle^{LAB} / cm^{-1}$	$NO(\langle v_2 \rangle)$
0	0	200	110	16–18
1	1,876	4,000	690	15
3	5,540	>4,000	1,350	11
10	17,600	not determined	1,280	⩽4
15	26,145	4,000	700[a]	1
16	27,600	3–4,000	⩾1,600	0

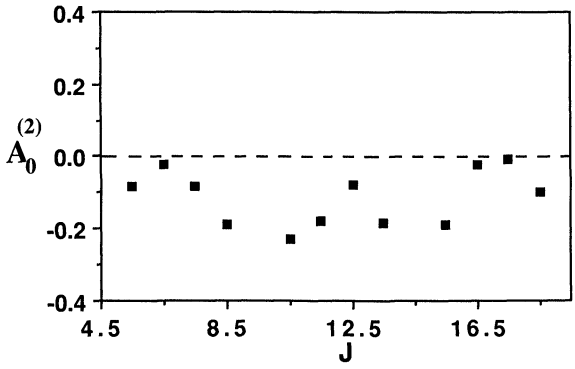

Figure 5 Rotational alignments for NO($v = 0$) generated in the reaction of velocity aligned O(^{1}D) with N_2O.

forward scattered partners, NO($v \sim 16$–18) are endowed with much higher LAB velocities, $\mathbf{V}_{NO} \geqslant 1.52$ km s^{-1} (for stripping dynamics $\mathbf{V}_{NO} \geqslant 2\,\mathbf{V}_{CM} \simeq 1.8$ km s^{-1}). The NO molecules excited into intermediate vibrational levels also have larger Doppler widths but their resolved parallel and perpendicular detection profiles are identical within experimental precision (see Figure 4(d)) implying a near isotropic angular distribution, with $\langle P_2(\hat{\mathbf{k}} \cdot \hat{\mathbf{k}}')\rangle \simeq 0$, and the intermediacy of a short-lived collision complex in the channels leading to vibrationally excited NO pairs.

Acknowledgements

R. Sayos thanks the British Council and the Spanish Ministry of Education and Science for the award of a Fleming Fellowship, P. A. Enriquez also thanks the Spanish Ministry of Education and Science for postgraduate research support.

References

1. "Orientation and Polarisation Effects in Reactive Collisions," Faraday Symposium, *J. Chem. Soc. Faraday Trans.* **2**, 1989, **85**, 925–1376.
2. R. N. Dixon, *J. Chem. Phys.* **95**, 1866 (1986).
3. J. P. Simons, *J. Phys. Chem.* **91**, 5378 (1987).
4. G. E. Hall and P. L. Houston, *Ann. Revs. Phys. Chem.* **40**, 375 (1989).
5. G. W. Johnston, S. Satyapal, R. Bersohn and B. Katz, *J. Chem. Phys.* **92**, 206 (1990); B. Katz *et al. Faraday Discussion Chem. Soc.* **91** (1991) in press.
6. F. Green, G. Hancock and A. J. Orr-Ewing, *Faraday Discussion Chem. Soc.* **91** (1991) in press; F. Green *et al. Chem. Phys. Lett.* (1991) in press.
7. M. Brouard, S. P. Duxon, P. A. Enriquez, R. Sayos and J. P. Simons, *J. Phys. Chem.* (1991) in press.
8. R. N. Zare, "Angular Momentum: Understanding Spatial Aspects in Chemistry and Physics," Wiley-Interscience: New York 1988.
9. K.-H. Gericke, R. Theinl and F. J. Comes, *J. Chem. Phys.* **92**, 6548 (1990).
10. J. J. Chu, P. Marcus and P. Dagdigian, *J. Chem. Phys.* **93**, 257 (1990).